

Experimental and numerical modeling of chemical osmosis in the clay samples of the aquitard in the North China Plain

Xiaomin Sun^{1,2} · Jianfeng Wu^{1,2} · Xiaoqing Shi^{1,2} · Jichun Wu^{1,2}

Received: 21 March 2015 / Accepted: 10 August 2015 / Published online: 21 December 2015
© Springer-Verlag Berlin Heidelberg 2015

Abstract This study focuses on addressing the existence of chemical osmosis in the clay samples of the aquitard in the North China Plain (NCP). For this purpose, chemical osmotic experiments in the clay samples collected from the aquitard in the NCP were implemented to estimate the reflection coefficient or chemico-osmotic efficiency in clayey sediments. More specifically, under a certain chemical potential gradient, the reflection coefficients were, respectively, achieved by measuring the osmotic flow and the induced pressure in terms of the two sets of undisturbed clay core samples and their remolded clay samples equipped in a rigid wall permeameter. The measured reflection coefficient is the value of 0.023 for in situ clay sample, much smaller than that of 0.098 for remolded sample. Also, the constant-head tests for determining the hydraulic conductivity of clay samples were conducted before and after the osmotic tests. It is indicated that the permeability of the remolded sample is smaller than the undisturbed sample in both periods. Moreover, a chemical osmosis continuum model was used to fit the evolution of the osmotically driven hydraulic pressure in the clay samples where more intrinsic parameters of the samples were calibrated. Additional analysis demonstrates the sensitivity of the osmosis pressure to the different parameters input to the model for the in situ clay sample. This study could provide a reliable basis for further evaluating the role of clay sediments in the desalination of shallow

saline groundwater and salinization of deeper fresh groundwater in the NCP.

Keywords Chemical osmosis · Reflection coefficient · In situ clay sample · Remolded clay sample · Continuum model

Introduction

Sediments with high clay content often show the properties of semi-permeable membrane. Sediments in regions with low permeability and concentration gradient can lead to chemical osmosis, thus resulting in osmotic flow and abnormal hydraulic head pressure (Olsen 1969; Barbour and Fredlund 1989; Neuzil 2000; Cey et al. 2001; Keijzer and Loch 2001; Malusis et al. 2003; Loch et al. 2005, 2010; Takeda et al. 2014). Chemical osmosis is of great importance to environmental science and geotechnical engineering. Chemical osmosis effect shows the significant impact on water flow, pore water pressure, and solute transport in the soil and chemical environment with low permeability. Therefore, the studies of membrane properties of clayey soils are of important theoretical significance to the clay barrier design for controlling salt water intrusion in offshore areas, waste landfills, and contaminated sites. Moreover, the studies of viscous soils are of practical value in cleaning contaminated soil and borehole stability applications.

The semi-permeable membrane ability is usually quantified in terms of the chemico-osmotic efficiency (Malusis and Shackelford 2002; Malusis et al. 2003; Yeo et al. 2005) or reflection coefficient (Kemper and Rollins 1966; Keijzer et al. 1999; Keijzer and Loch 2001). For the ideal clay medium which can completely restrain solute, the

✉ Jianfeng Wu
jfwu@nju.edu.cn; jfwu.nju@gmail.com

¹ Key Laboratory of Surficial Geochemistry, Ministry of Education, Nanjing University, Nanjing 210023, China

² Department of Hydrosciences, School of Earth Sciences and Engineering, Nanjing University, Nanjing 210023, China

reflection coefficient is equal to 1; for the clay medium with non-selective semi-permeable membrane efficiency, the reflection coefficient is equal to 0, indicating that the chemical osmosis does not exist. In reality, the coefficient of the chemical osmosis efficiency for the clay media is generally between 0 and 1.

In many laboratory tests, the determination of chemical osmosis efficiency coefficient of remolded clay confirmed that clay was characterized by the semi-permeable membrane efficiency (Marine and Fritz 1981; Fritz and Marine 1983; Barbour and Fredlund 1989; Keijzer and Loch 2001; Olsen 2003; Malusis and Shackelford 2004; Hart et al. 2008; Kang and Shackelford 2009; Oduor et al. 2009). Through laboratory tests of bentonite and compacted dredged mud (clay mass fraction of 56 %), Keijzer and Loch (2001) observed chemical osmosis phenomenon and the measured chemical osmosis efficiency coefficient was, respectively, 0.015–0.030 and 0.019–0.022. In the mud with clay mass fraction of 26 %, the chemical osmosis phenomenon was not observed, indicating that chemical osmosis efficiency was decreased or even declined to zero with the decreasing clay content. Moreover, Fritz and Marine (1983) found that chemical osmosis efficiency coefficient of sodic expansive soil reached 0.89 under the low porosity and low concentration gradient. On the contrary, chemical osmosis efficiency coefficient reached 0.042 under the high porosity and concentration gradient. Similarly, other researchers (Malusis and Shackelford 2002; Yeo et al. 2005) carried a series of multiple-stage chemico-osmosis tests and found chemical osmosis efficiency coefficient gradually decreased when KCl concentration gradient between the two ends of clay samples was gradually increased. The results indicated that pore water concentration would affect clay membrane efficiency and the chemical osmosis efficiency coefficient decreased with the increasing of pore water concentration. In some other laboratory tests, undisturbed *in situ* clay also showed the semi-permeable membrane effect (Cey et al. 2001; Oduor and Whitworth 2004; Henning et al. 2006). With undisturbed soil samples from the soil depth of 88–123 m, Cey et al. (2001) quantitatively analyzed chemical osmosis capability through the measurements of hydraulic gradient and volumetric change within certain concentration range and obtained the chemico-osmotic efficiency (or reflection coefficient) ranging from 0.0028 to 0.42. Henning et al. (2006) found that two kinds of expansive soil from the construction sites in New Jersey and Delaware showed the membrane performance which was equivalent to the membrane performance of remolded soil. The membrane performance increased with the decrease of porosity and the increase of clay content. Field evidences of the clay semi-permeable membrane efficiency were shown in the form of the abnormal hydraulic head pressure in the clay-

rich sedimentary basins (Hanshaw and Hill 1969; Hanshaw 1971; Kharaka and Berry 1974; Marine and Fritz 1981; Fritz 1986). Recently, Neuzil (2000) drilled four wells in Dakota shale (pore water content of 3.5 g/L) in Middle America and added water solutions with different concentrations (35 g/L for two solutions; 3.5 g/L for one solution; deionized water for another) into various wells. Neuzil (2000) monitored water table and total dissolved solids (TDS) in the wells for 9 years and found that heads in the wells with saline water increased to a maximum of 2 m compared to the one with duplicate pore water due to chemical osmosis effect. The monitoring results provided the direct field test proof for chemical osmosis effect. Similarly, Noy et al. (2004) suddenly changed water concentration in Jurassic clay in a stabilized sealed well in Switzerland observed the significant change in hydraulic head pressure, providing the similar direct field evidence of the clay semi-permeable membrane effect.

The assessment methods of clay membrane efficiency were mostly established on the Donnan Equilibrium Concept, the Teorell–Meyer Filtration Theory and the Gouy–Chapman Theory of the Diffuse Double Layer (Keijzer 2000). The assessment methods were proposed to explore the influences of clay porosity, geometric model (shapes and arrangement of the clay particles), cation exchange capacity (CEC) of the clay, the water film thickness of the clay particles, and the clay pore water concentration on clay membrane efficiency. The chemical osmosis models considering complex fluid flow and solute transport included the discontinuous model (Yeung 1990; Yeung and Mitchell 1993; Olsen et al. 2000) and continuous model (Greenberg et al. 1973; Sherwood and Craster 2000; Soler 2001; Garavito et al. 2002, 2006; Malusis and Shackelford 2002; Ghassemi and Diek 2003; Kooi et al. 2003; Bader and Kooi 2005). In the discontinuous model, the membrane efficiency was usually evaluated through the determination of pressure gradient across the clay and the concentration difference (including constant flow rate state and non-flow state). This evaluation method has been widely used in the calculation of the average membrane efficiency. The continuous equation is usually derived from unbalanced thermodynamic status. Considering the impact of concentration gradient on the osmotic flow, combined with flow and solute conservation equation, a set of differential equations can be obtained to simulate and predict the changes of solute concentration and hydraulic head pressure with time and space. Greenberg et al. (1973) developed a one-dimensional model for characterizing the coupled salt and water flows in the embedded solid layer of Oxnard Basins in California, the United States. In the embedded solid layer, chemical consolidation led to the sedimentation as well as seawater intrusion into adjacent aquifers (Datta et al. 2009). Soler (2001) carried out simple one-

dimensional transport simulation including thermal and chemical osmosis, hyperfiltration and thermal diffusion to study the radionuclide transport from a repository of nuclear waste in the Opalinus Clay, Switzerland. Sherwood and Craster (2000) proposed the three-parameter controlled transient flow model to interpret testing results of clay membrane performance and simplified transport behaviors of water flow and solutes passing through the clay membrane. Malusis and Shackelford (2002) proposed a complex continuous transfer model for the exchange among various anions or cations. Through the comparison of the chemical osmosis testing data and the data obtained with conventional convection–dispersion equations and the model, it was found that the data obtained with the model were consistent with testing results. The model can only interpret the result for the case of the chemical osmosis efficiency coefficient equal to zero. Thus, this model cannot reflect the relationship between the coefficient of chemical osmosis efficiency and the concentration of solutions.

This paper is intended to investigate the existence of chemical osmosis in the aquitard where is the vertical mixing zone between the shallow aquifer containing saline groundwater and the deeper aquifer containing fresh groundwater in the North China Plain (NCP) and to further determine the coefficient of chemical osmosis efficiency associated with the aquitard of interest. To achieve the goal, clay samples including in situ and remolded samples collected from the aquitard of interest and subjected to chemical osmosis experiments. Moreover, based on the monitoring chemical osmotic pressures in the experiments, the numerical simulation model for fluid flow and solute transport in the clay samples is conducted to identify the intrinsic parameters of clay. This work provides the reliable basis for further evaluating the effect of the chemical osmosis in clayey sedimentary aquitards on the desalination of shallow saline groundwater and salinization of deeper fresh groundwater in the NCP.

Experimental design and testing procedures

Sampling site

The sampling site, a groundwater test base of Ministry of Land and Resources of China, is located at Shenzhou County of Hengshui City, Hebei Province in the NCP (Fig. 1). The topography is alluvial-proluvial plain with flat terrain and the elevation of about 20 m above sea level. Geographic position of the test base is bounded by latitude $37^{\circ}54'21.5''$ – $37^{\circ}54'26.5''$ north, and longitude $115^{\circ}40'42.3''$ – $115^{\circ}40'49.3''$ east. The study area is characterized by the complicated geological and hydrological conditions. Groundwater can be vertically divided into five

groups of aquifers from top to bottom. The uppermost aquifer is unconfined aquifer group containing highly mineralized salt water; and the other four aquifer groups contain deep confined fresh water. The test base is a representative location for investigating the downward movement of shallow saltwater in NCP. Many previous studies (Fei 1988; Wang et al. 2008, 2012; Cao et al. 2013) have focused on the investigation of the hydrogeological and hydraulic mechanisms related to the downward movement of saltwater in the NCP. However, the role of chemical osmosis phenomenon has never been discussed in renewability and sustainability of groundwater resources in the NCP.

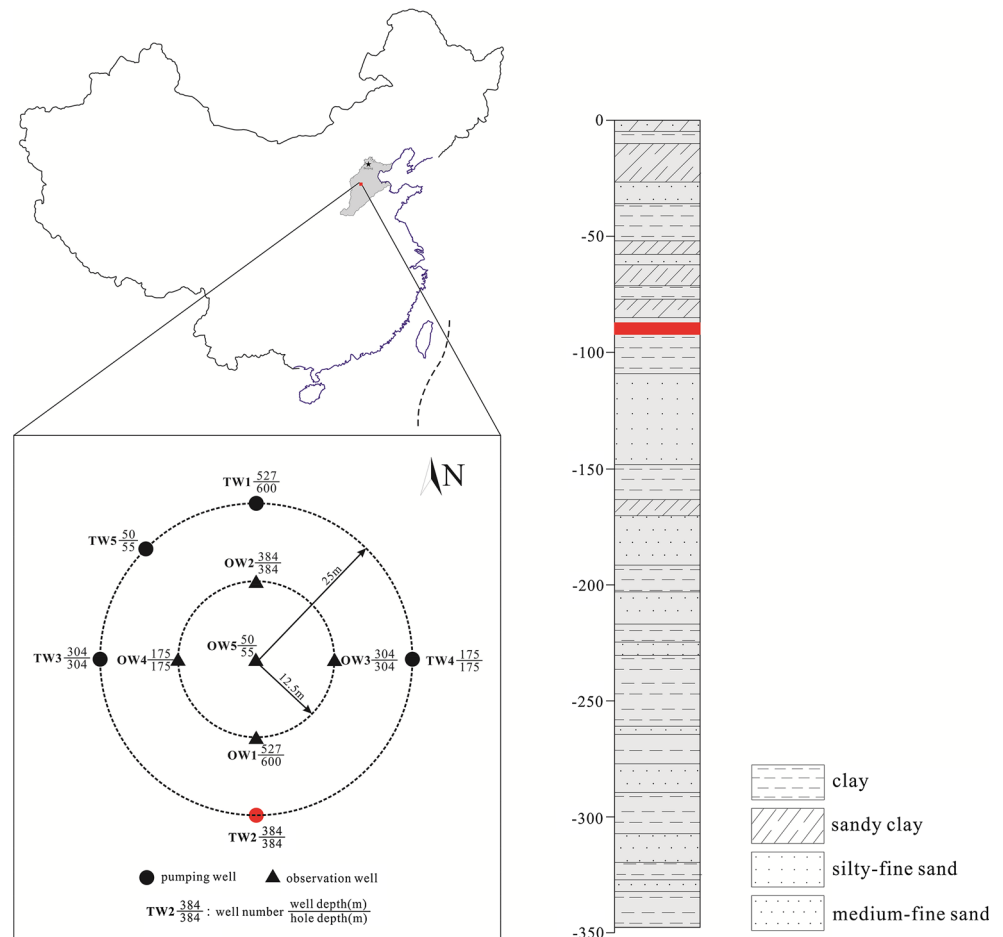
Experimental design and testing procedures

The used clay samples in the experiments were the Pleistocene clayey sediments taken from sample cores of Shenzhou borehole TW2 at depth 87.1–87.3 m below ground surface (Fig. 1). The clayey sediments at this depth form the aquitard between the shallow aquifer (Aquifer 1) containing saline groundwater and the deeper aquifer (Aquifer 2) containing fresh ground water in the area. For the sake of simplicity, the salt water solution selected in the experiments was tested with 8.9 g/L (0.152 mol/L) NaCl solution, approximately equivalent to the maximum TDS of the groundwater in the concerned shallow aquifer.

In the experiments, the reflection coefficient σ was evaluated through the measurement of water flow and abnormal hydraulic head caused by chemical potential gradient in the clay. The experimental device as illustrated in Fig. 2 is composed of a permeameter and two connected reservoirs. The permeameter consists of three parts: two end caps and one O-ring (a mechanical gasket designed in a toric shape). These three parts are fixed together to form a unified whole with four stainless steel screws. Each end cap contains one chamber which can accommodate one piece of 1.5-cm-thick porous stone with the diameter of 5 cm. Each end cap is equipped with two ports which are connected via one peristaltic pump and reservoirs to form and maintain the constant chemical potential gradients at both ends. Each reservoir is equipped with the devices as follows:

- (1) A scaled burette to measure the water exchange capacity between the two reservoirs;
- (2) a pressure sensor to monitor pressure changes inside the reservoir;
- (3) a pressure valve to limit the maximum pressure inside the reservoir;
- (4) a pressure port to control the pressure inside the reservoir to simulate the burial pressure environment of clay samples;
- (5) a low-flow peristaltic pump for water exchange between end cap and the reservoir; and
- (6) a pressure difference sensor was fixed to detect the pressure

Fig. 1 The location of the sampling well (red-filled circle) at the test base site in the North China Plain and the geological profile of the sampling well showing the position of clayey sediments (red-filled) sampled for the experiment



difference between the two reservoirs. Moreover, the whole equipment is placed in the environment with a temperature between 18 and 22 °C to prevent temperature gradient affecting the sensor accuracy. Under this temperature condition, the measurement error of the pressure sensor caused by the temperature is less than 1 % of relative error and should be neglectable accordingly.

To begin the experiments, the clay samples must be properly loaded into the permeameter and fixed with bolts (see Fig. 2). The in situ clay was carefully cut into the proper size. Then the remaining clay was cut into remolded samples with the identical size and porosity.

The experimental procedure can be briefly described as follows. First of all, circulating distilled water was supplied at both ends of the sample to saturate clay samples and remove the dissolved salts in clay samples. Then the hydraulic conductivity of clay samples was measured before and after the chemical osmosis test. In this study, the falling head method is used for measurement of the hydraulic conductivity of clay samples. In this method, a constant pressure of 10 kPa is added at one end of the reservoir under the same solution concentration of both

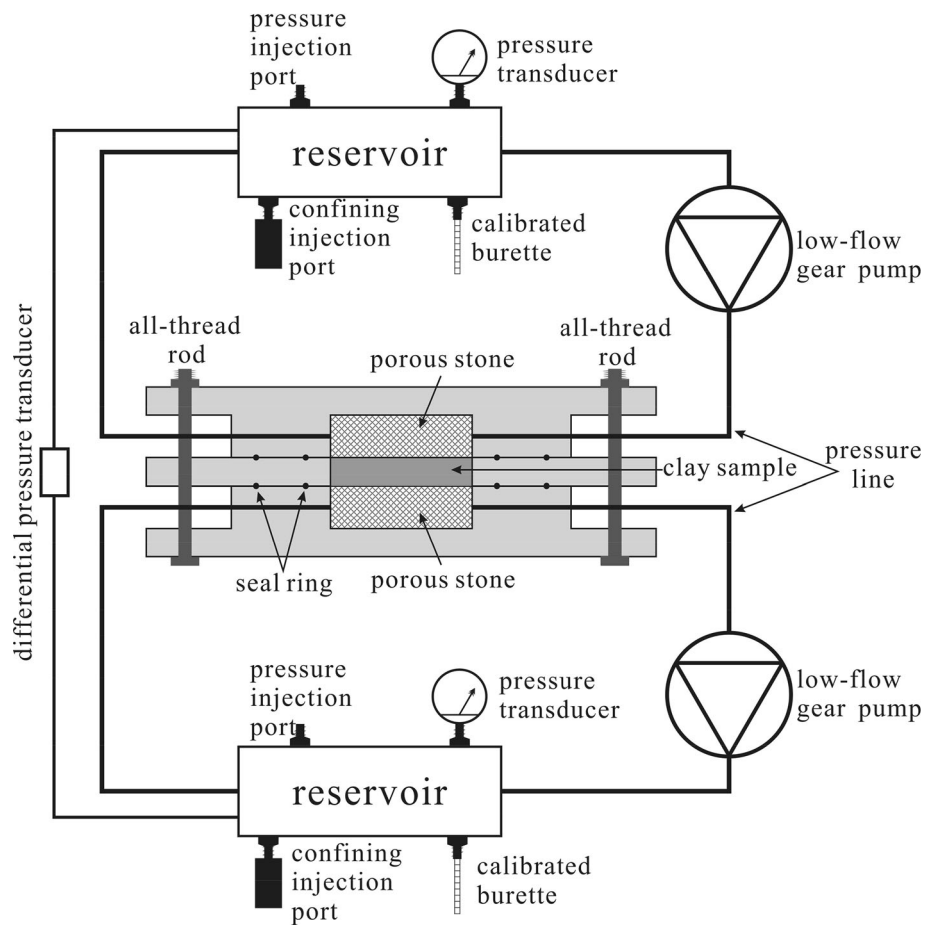
ends, and the water flow through the clay sample can be measured by the burette installed on another end of the reservoir. More detailed measurement of hydraulic conductivity of clay with low permeability can be read from Daniel (1984), Dunn and Mitchell (1984), and Benson and Daniel (1990).

Following the measurement of hydraulic conductivity of clay, chemical osmosis test consists of two stages: the open reservoir stage and the closed reservoir stage. In both stages, water flow circulation on one end was replaced by the 8.9 g/L NaCl solution. Water flow (in the open reservoir stage) and abnormal pressure (in the closed reservoir stage) is considered to be caused by the concentration gradient. The osmotic pressure can be theoretically calculated by the van't Hoff equation (Katzir-Katchalsky and Curran 1965):

$$\Delta\pi = \nu RT\Delta C, \quad (1)$$

where $\nu [-]$ is the ion type ($\nu = 2$ for NaCl); R [J/(mol K)] is the thermodynamic constant (8.314); T [K] is the absolute temperature; ΔC [mol/L] is the concentration difference. In this study, $\Delta\pi$ was calculated to be 682 kPa.

Fig. 2 Schematic diagram of testing apparatus: the equipment package includes a rigid wall permeameter connected with two stainless steel reservoirs. The hydraulic conductivity of clay samples was obtained by measuring the water flux and the hydraulic gradient between two reservoirs. Solutions of different concentrations were added to the reservoirs, respectively, to achieve a certain chemical potential gradient. The chemical reflection coefficient, σ , was estimated by measuring the water flux (open reservoir phase) and abnormal pressure caused by the chemical potential gradient



Results and discussion

The measurement results of the clay permeability are shown in Table 1. For the two sets of samples, the results measured before the chemical osmosis experiments were lower than those measured after the same experiments. First, the increasing water concentration after the test completion lowers the dynamic viscosity and increases clay permeability. Afterward, the

Table 1 Clay permeability and chemical osmosis coefficient

Sample for test	Parameter value measured by the tests			
	$k (\times 10^{-19} \text{ m}^2)$		$\sigma (-)$	
	Before*	After	Open**	Closed
In situ clay	23 ± 5	37 ± 6	0.011 ± 0.0025	0.023
Remolded clay	8.9 ± 1	9.1 ± 2.1	0.083 ± 0.0092	0.098

* “Before” and “after” denote the measured permeabilities before and after the chemical osmosis experiments, respectively. “ 23 ± 5 ” means the parameter value is the average of 23 with a deviation ranging from -5 to $+5$

** “Open” and “closed” denote the reflection coefficients obtained in the stages of open and closed salt water reservoirs, respectively

increasing pore water concentration leads to flocculation effect in clay particles, which facilitates the liquid to pass through clay samples. In the two samples, the permeability of in situ clay was significantly higher than that of remolded clay before and after the test because the sorting of clay particles became better after clay remodeling for the remolded clay.

As expected, the two samples showed the membrane efficiency under concentration gradient. In the rigid wall permeameter, the change of clay volume can be ignored. Chemical osmosis reflection coefficient can be calculated by Eq. 2 (Katzir-Katchalsky and Curran 1965):

$$\sigma = \frac{\Delta P}{\Delta \pi}, \tag{2}$$

where $\sigma [-]$ is the reflection coefficient; ΔP [Pa] is the directly or indirectly measured real osmotic pressure caused by the chemical concentration gradient.

In the open stage of the reservoir, ΔP was determined by measuring water flow driven by the osmotic pressure. It is assumed that hydraulic head gradient is negligible and only chemical concentration gradient exists, ΔP was determined with the Darcy’s Law (Barbour and Fredlund 1989; Keijzer et al. 1999; Keijzer and Loch 2001):

$$\Delta P = \frac{\rho g J_w d}{K_h A} = \frac{\mu J_w d}{k A}, \quad (3)$$

where ρ [kg/m³] is the fluid density; g [m²/s] is the gravitational acceleration; d [m] is the clay thickness; K_h [m/s] is the hydraulic conductivity; A [m²] is the area of the samples; μ [Pa s] is dynamic viscosity; k [m²] is the intrinsic permeability. The obtained reflection coefficients of chemical osmosis are shown in Table 1.

After the open reservoir stage, two reservoirs were replaced by the initial solution. Then the salt water reservoir was closed. The changes of pressure in the salt water reservoir (colored dots) caused by the chemical concentration gradient are shown in Fig. 3a, b.

As shown in Fig. 3a, b, the osmotic pressure caused by the chemical concentration gradient on both ends rapidly increased with time. Then the osmotic pressure reached the maximum value and declined gradually. Although the two clay samples have the same porosity, osmotic pressure measured in in situ sample reaches its maximum value earlier than that recorded in remolded sample and the maximum value in in situ clay is significantly lower than that in remolded clay. The difference of osmotic characteristics between the in situ clay sample and remolded clay

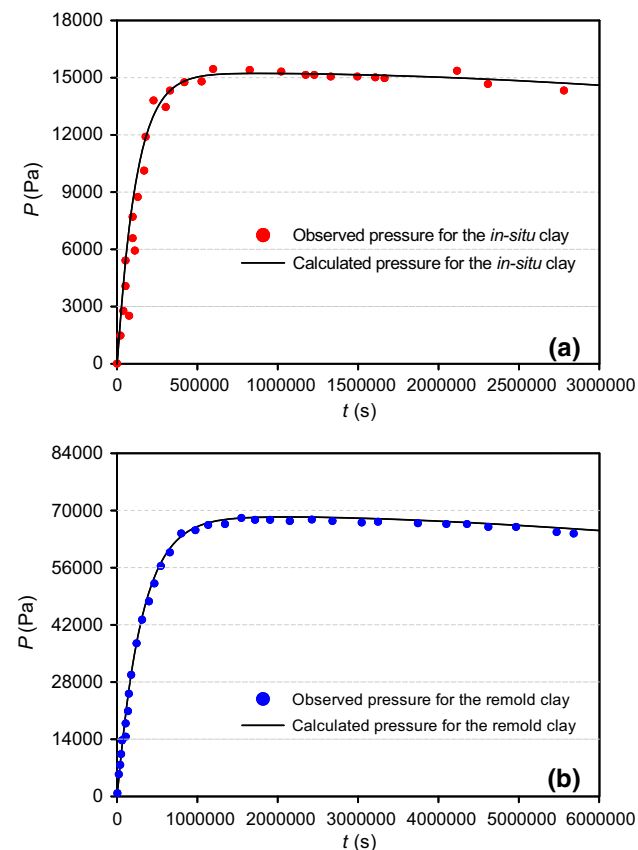


Fig. 3 The evolution of pressures in salt water reservoir (P) for **a** in situ sample, and **b** remolded sample

samples originates in their difference in clay particle arrangement. The particle arrangement in in situ clay samples is more complex and there often contains large pores or tiny fractures (Dunn and Mitchell 1984). This particle arrangement may increase the permeability of clay samples, lower the chemical osmosis efficiency, and even decrease the clay membrane efficiency.

The osmotic pressure slowly decreased after reaching the peak value, indicating that clays with chemical osmosis are non-ideal semi-permeable membranes and then the solute cannot be completely blocked by the clay samples. During the test, due to the dispersion effect, the high concentration of ions gradually entered the reservoir with low concentration of ions through the clay samples. Thus, chemical potential gradient on both ends of the clay sample was decreasing and the corresponding chemical potential was also decreasing. On the other hand, due to the flocculation of clay particles, the electrical double layers attached to the clay particles were contracted so that ions can pass through the clay samples more easily.

As shown in Table 1, the reflection coefficients (σ) of chemical osmosis are different in the two stages. The value of σ measured in the open stage is slightly less than that in the closed stage. The results can be interpreted as follows. During the open stage, water was exchanged between the two reservoirs and ions entered the reservoir with the low ion concentration. On the contrary, in the closed stage, water was not exchanged between the two reservoirs and ions entered the reservoir through the ion diffusion.

Numerical simulation of chemical osmosis effect

Numerical modeling of chemical osmosis

The determination of chemical osmosis efficiency coefficient is based on the previously described discontinuous model (Yeung 1990; Yeung and Mitchell 1993; Olsen et al. 2000; Malusis et al. 2003), which is unable to reflect the change of pressure or concentration. Therefore, we adopted the complex liquid flow and solute transport model proposed by Garavito et al. (2006) to interpret the chemical osmotic pressure curve observed in the experiment.

The model is derived from the unbalanced thermodynamics equation. In the unbalanced thermodynamics theory, different types of water flow J_i are driven by different potentials (Bader and Kooi 2005):

$$J_i = \sum_{j=1}^n L_{ij} x_j, \quad (4)$$

where L_{ij} are the coupling coefficients that relate flows of type i to gradient of type j . Since the model considers only

the hydraulic head gradient and chemical potential gradient, constitutive equations of the fluid and solute are as follows:

$$J_v = \frac{k}{\mu} (\nabla \rho_0 g h - \sigma \nabla \pi) \tag{5}$$

$$J_s^m = -D(1 - \sigma) \nabla(\rho \omega) + (1 - \sigma) \rho_f \omega J_v, \tag{6}$$

where J_v [m^3/m^2s] and J_s^m [kg/m^2s] are the water flow and solute mass flow, respectively; h [m] is the hydraulic head; D [m^2/s] is the diffusion coefficient; ω [-] is the mass fraction of the solution; ρ_f [kg/m^3] is salt water density.

On the right hand side of Eq. 6, the first item is the diffusion item; the product $\sigma \rho_f \omega J_v$ is the ultrafiltration item. If $\sigma = 0$, the membrane efficiency does not exist and the equation can be simplified as the traditional advection–diffusion equation; if $\sigma = 1$, then $J_s^m = 0$, which is the same as with the fact that solute transport is completely blocked by an ideal membrane.

The mass conservation equations are given by:

$$\frac{\partial(n\rho_f)}{\partial t} + \nabla(\rho_f J_v) = 0 \tag{7}$$

$$\frac{\partial(n\omega\rho_f)}{\partial t} + \nabla J_s^m = 0. \tag{8}$$

Substituting the constitutive equations given by Eqs. 5 and 6 into the mass conservation equations given by Eqs. 7 and 8, we can derive the partial differential equations describing the solute concentration and pressure with time and space, respectively.

For this particular experiment dealt with a one-dimensional problem, the governing differential equations can be stated as the following equations proposed by Bader (2005):

$$n_i S_{si} \frac{\partial P_i}{\partial t} = \frac{k}{\mu} \frac{\partial^2 P_i}{\partial x^2} - \theta_i \frac{\partial^2 C}{\partial x^2} \tag{9}$$

$$n_i \frac{\partial C}{\partial t} = D_i \frac{\partial^2 C}{\partial x^2}, \tag{10}$$

where the composite parameter $\theta = (\sigma k/\mu)RTv$ is dependent on a series of parameters; S_s [m^{-1}] is the specific storage, the subscript i is an identifier for the different subdomains of the experiment domain (see Fig. 4), representing the parts I, II, and III for $i = 1, 2,$ and $3,$ respectively.

As mentioned above and shown in Fig. 4, the experiment domain based on the closed reservoir stage is divided into three parts: two porous stone areas and one sample area. The porous stone on the left side (I, 0–0.015 m) was soaked with circulating distilled water ($C = 0$); the porous stone on the right side (III, 0.025–0.04 m) was soaked with NaCl (0.152 mol/L); the middle part between the left and right porous stones was filled with the clay sample (II,

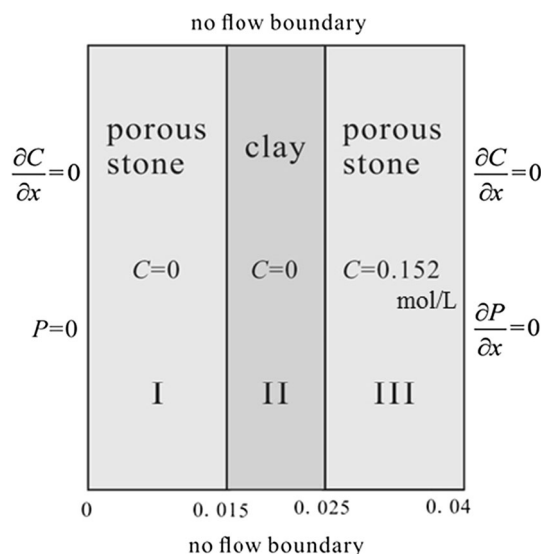


Fig. 4 Model configuration and initial and boundary conditions for the experiment

0.015–0.025 m). As pointed out above, circulating distilled water was supplied on both sides of the samples before chemical osmosis test. Also, the pore water concentration in clay sample can be considered to be 0.

For the one-dimensional numerical model, the boundary conditions based on the conceptual model as in Fig. 4 can be mathematically stated as:

$$\begin{cases} \frac{\partial C_1}{\partial x} = 0 \\ P_1 = 0 \end{cases} \text{ for } x = 0 \tag{11}$$

$$\begin{cases} \frac{\partial C_3}{\partial x} = 0 \\ \frac{\partial P_3}{\partial x} = 0 \end{cases} \text{ for } x = 0.04. \tag{12}$$

The corresponding initial conditions of the model can be expressed as:

$$P(x, 0) = 0 \text{ for } x \in [0, 0.04] \tag{13}$$

and

$$C(x, 0) = \begin{cases} 0 & \text{for } x \in [0, 0.025] \\ 0.152 & \text{for } x \in [0.025, 0.04] \end{cases}. \tag{14}$$

Equations 9–14 above define a one-dimensional mathematical model that reflects the chemical osmosis effect that existed in the clay sample. On the basis of work of Bader (2005), the analytical solution for the pressure to this model in the clay can be therefore derived as:

$$P(x, t) = A \operatorname{erfc} \left(\frac{-d}{2\sqrt{\frac{k_2 t}{\mu n S_{s3}}}} \right) - B \operatorname{erfc} \left(\frac{-d}{2\sqrt{D_2 t}} \right), x \in [0.025, 0.04] \tag{15}$$

with

$$A = \frac{\lambda C_3 \mu}{k_2} \left(1 + \frac{\sqrt{S_{s3} \mu D_1 k_2}}{k_3} \right), B = \frac{\lambda C_3}{\left(\frac{k_2}{\mu} - S_{s3} D_2 \right) \left(1 + \frac{k_2}{k_3} \right)}, \quad (16)$$

where the subscripts 2 and 3 similarly denote the subdomains 2 (clay) and 3 (porous stone) of modeled domain, respectively. Again, considering $k_2 \ll k_3$, Eq. 16 can be simplified to as follows:

$$A = \frac{\lambda C_3 \mu}{k_2}, B = \frac{\lambda C_3}{\left(\frac{k_2}{\mu} - S_{s3} D_2 \right)}. \quad (16')$$

Actually, the pressure measured by the sensor inside the reservoir (the right porous stone) corresponds to the solution of Eq. 15 at $x = 0.025$. As shown in Table 1, some parameters required for numerical simulation are the pre-determined parameters, including the intrinsic permeability k , the porosity n , and the reflection coefficient σ . It is assumed that these pre-determined parameters are fixed during the whole experimental period. The other unknown parameters for numerical simulation, including the diffusion coefficient (D) and the specific storage (S_s), are given reasonable initial values as suggested by Bader and Kooi (2005). Generally, the value of specific storage (S_s) for the porous stone is greater than that for the clay sample, so is the value of diffusion coefficient (D). In this study, it is shown that the simulation results are very insensitive to the specific storage (S_s) of clay sample and diffusion coefficient (D) of porous stone, as long as the values of the parameters are set in a reasonable range. On the other hand, the specific storage (S_s) of porous stone and the diffusion coefficient (D) of clay sample can be achieved by fitting the experimental data. The calibrated parameters input to the model are listed in Table 2.

An excellent match between the measured pressures (colored dots) and the calculated curve output by Eq. 15 (continuous line) as shown in Fig. 3 indicates that this model can be used to explain the evolution process of the

pressure in the experiments. Of course, the model can also be used to simulate the evolution of concentration over time. However, concentration measurement elements are not provided in the test, the concentration change is not available for this study.

Sensitivity analysis

Shown in Fig. 5 are the qualitative changes of the pressure for the in situ clay samples estimated by Eq. 15 dependent on the several main parameters over time. Comparatively, the parameter σ mainly affects the peak value of the osmotic pressure, while the parameter D mainly affects the decay rate of the late pressure curve over time. It is noteworthy that the decay rate of the osmosis pressure over a period of time is referred to as the ratio of its decrease from the peak in pressure to the duration of the period. Also, the clay intrinsic permeability (k) and specific storage of porous stone (S_s) similarly dominate the arrival time to the peak of osmotic pressure. Actually, it is too complicated to discriminate how the pressure curve is controlled by the individual parameters on earth. For example, both of the clay intrinsic permeability (k) and specific storage of porous stone (S_s) not only control the duration required for reaching the osmotic pressure peak, but also affect the peak value of the osmotic pressure to a certain extent (Bader 2005; Garavito et al. 2006). Moreover, various parameters are mutually affected. For instance, the value of k definitely affects the value of σ .

On the basis of the qualitative analysis of model parameters for the in situ clay samples, we further used the deterministic sensitivity analysis to quantitatively evaluate the importance of different parameters in the established model on the osmotic pressure. Shown in Fig. 6 are the results of sensitivity analysis based on perturbations of the parameters ranging from -50 to $+50$ %. As shown in Fig. 6a, among these model parameters, including the reflection coefficient (σ), diffusion coefficient (D), intrinsic permeability (k), and the specific storage (S_s), the per-

Table 2 The calibrated parameters input to the models for the in situ and the remolded clay samples in the chemical osmosis experiments

Item	Parameter value in different model subdomain		
	Parts I and III (porous stone)	Part II (in situ clay)	Part II (remolded clay)
n , porosity (–)	0.5	0.47	0.47
σ , reflection coefficient (–)	0	0.023	0.089
k , intrinsic permeability (m^2)	1.0×10^{-13}	23×10^{-19}	8.9×10^{-19}
D , diffusion coefficient (m^2/s)	1.0×10^{-10}	3.0×10^{-12}	1.2×10^{-12}
S_s , specific storage (m^{-1})	3.6×10^{-8}	1.0×10^{-8}	1.0×10^{-8}

It is assumed that these parameters are fixed during the whole experiment period. The values of porosity for the porous stone and the clay samples are pre-measured and considered constant

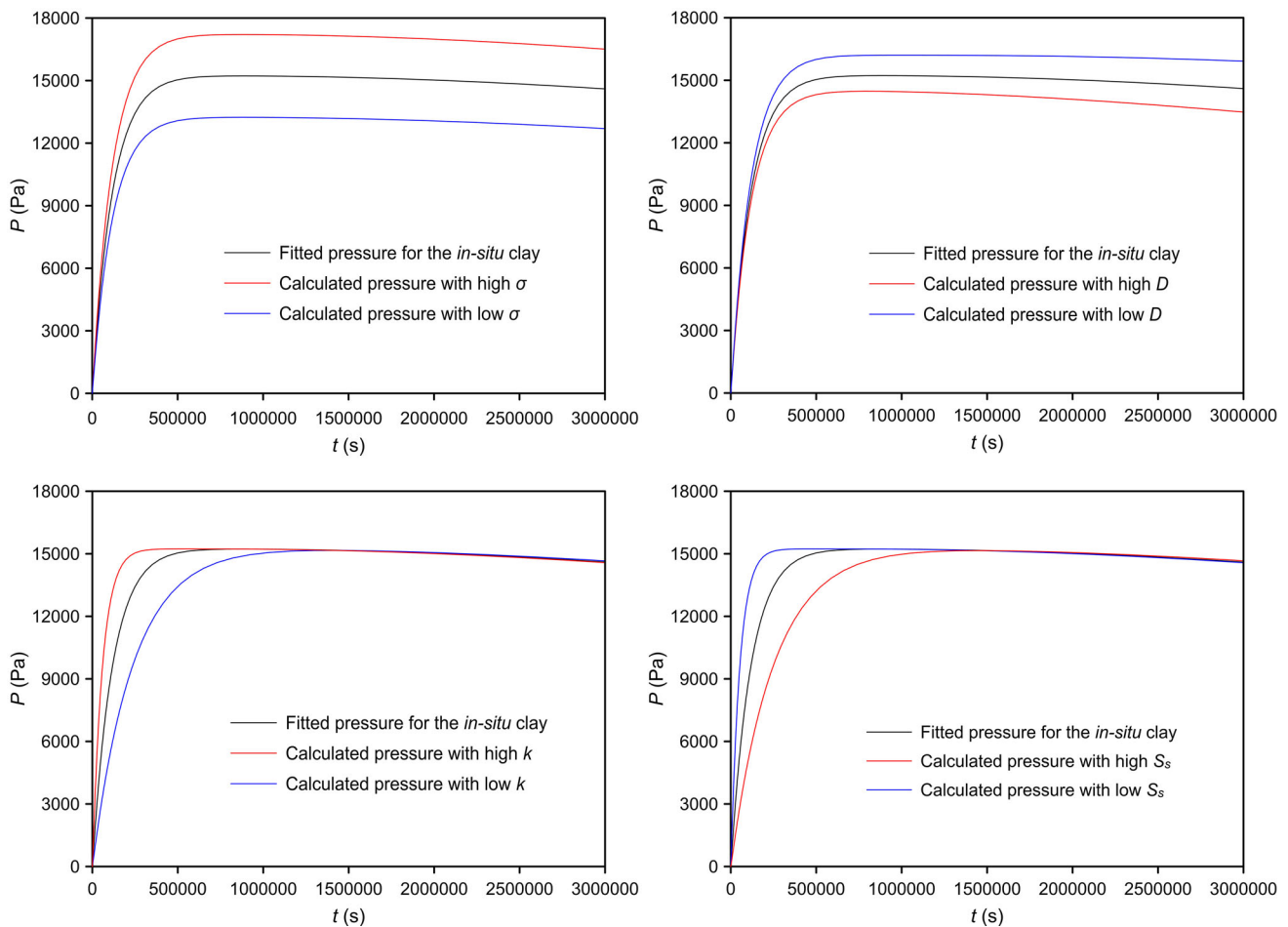


Fig. 5 Qualitative analysis of the osmosis pressure over time with respect to the different parameters for the in situ clay samples. Here, σ is the reflection coefficient, D is the diffusion coefficient, k is the intrinsic permeability, and S_s is and specific storage

centage change of σ results in the equivalent percentage change of the peak value of the osmosis pressure. Also, +50 or -50 % of D approximately leads to a change of the peak pressure with -5.08 or 7.56 %. However, +50 or -50 % of k and S_s hardly influences the peak pressure with its perturbation less than 1 %. Thus, the peak value of the osmosis pressure obtained from the model is highly sensitive to the reflection coefficient (σ), and insensitive to the other parameters. Similarly, Fig. 6b indicates that the decay rate of the pressure over a period of time is very sensitive to the diffusion coefficient (D) but insensitive to the other three parameters. In particular, as shown in Fig. 6c, we can infer that both of the intrinsic permeability (k) and the specific storage (S_s) profoundly influence the arrival time to the peak value of the pressure. On the contrary, both the reflection coefficient (σ) and diffusion coefficient (D) have nothing to do with the arrival time to the peak value of the pressure.

As mentioned above, the results of sensitivity analysis indicate that different individual parameter plays its importance in affecting the evolution of osmosis pressure over time in the experimental tests and the numerical modeling. Note that this study is only the first step toward a comprehensive effort to investigate the osmosis effect of the clay samples on the downward intrusion of saline groundwater in the NCP.

Conclusions

To investigate the existence of chemical osmosis in the aquitard between the shallow aquifer containing saline groundwater and the deeper aquifer containing fresh groundwater in the North China Plain (NCP), we chose clay samples including in situ and remolded samples collected from the aquitard of interest to carry out a series of chemical

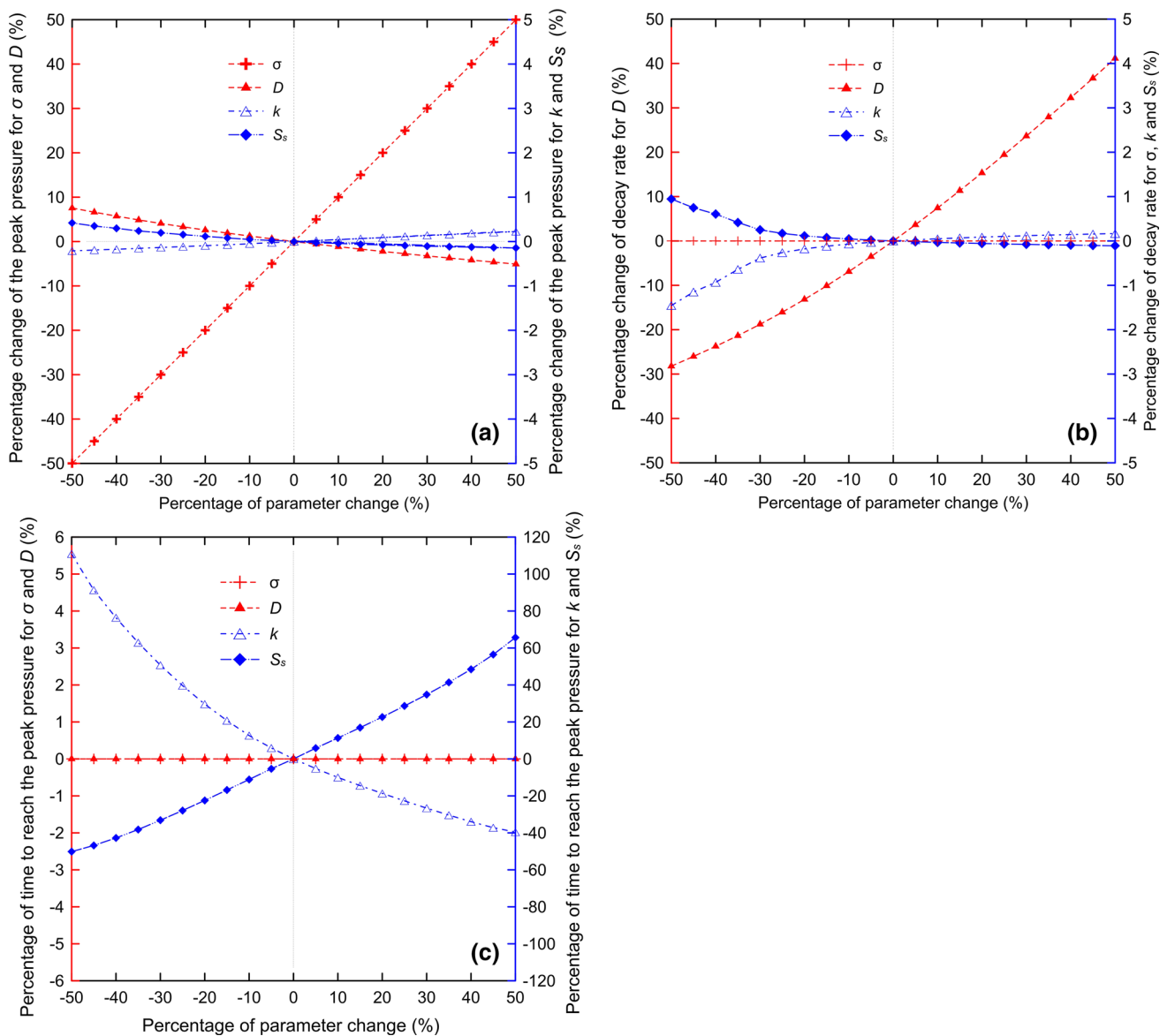


Fig. 6 Sensitivity analysis of the evolution of the osmosis pressure over time with respect to the reflection coefficient (σ), diffusion coefficient (D), intrinsic permeability (k), and specific storage (S_s) for the in situ clay samples

osmosis experiments. The experimental results show that apparent osmotic flow can be monitored, no matter what the clay sample for test is the in situ or the remolded. Meanwhile, the reflection coefficient (σ) measuring the magnitude of osmotic flow for the in situ and remolded clay are 0.011–0.023 and 0.083–0.098, respectively, by the open reservoir and closed reservoir methods. Obviously, compared with undisturbed (in situ) clay, remolded clay possesses a higher chemical osmosis efficiency coefficient (σ) and a lower permeability (k) because the sorting of clay particles became better for the remolded clay. Also, for both in situ and the remolded clay samples, the reflection coefficient measured in the open reservoir stage is smaller than that measured in the closed reservoir stage.

Moreover, a chemical osmosis continuum model was conducted to simulate the evolution of the osmotically driven hydraulic pressure in the clay samples. To identify the intrinsic parameters of clay, the simulating results output from the continuum model are compared with the measured data in the closed reservoir stage for the in situ clay sample experiment. An excellent match between the measured and the calculated pressure data indicated that the model can be used to simulate the transient evolution of fluid pressure induced by the chemical osmosis gradient. It is verified that the model is applicable to interpret a series of osmosis tests, including laboratory test and in situ field osmosis test. Sensitivity analysis indicates that the different individual parameters input to the model play their

importance in affecting the evolution of osmosis pressure over time. The reflection coefficient (σ) and the diffusion coefficient (D) mainly control the peak value and the decay rate of the osmosis pressure over a period of time, respectively. At the same time, both of intrinsic permeability (k) and the specific storage (S_s) profoundly influence the arrival time to the peak value of the pressure. In particular, this study indicates that the chemical osmosis phenomenon certainly occurs in clayey sediments between the shallow saline groundwater and deeper fresh groundwater in the North China Plain. This requires that the osmotic transport should be taken into account in the quantitative assessment of the hydrological process for the salt-rich region of the North China Plain (NCP). Furthermore, this study provides a reliable basis for further evaluating the effect of the chemical osmosis in the aquitard on the desalination of shallow saline groundwater and salinization of deeper fresh groundwater in the NCP.

Acknowledgments This work was supported by the National Basic Research Program of China (the “973” program, No. 2010CB428803) and the National Natural Science Foundation of China (Nos. 41372235, 41072175 and 41030746). We also would like to thank Prof. Zongyu Chen of Institute of Hydrogeology and Environmental Geology, Chinese Academy of Geological Sciences (CAGS), who kindly provided the in situ clay samples for the experimental tests. The numerical calculations in this paper have been implemented on the IBM Blade cluster system in the High Performance Computing Center of Nanjing University.

References

- Bader S (2005) Osmosis in groundwater: chemical and electrical extensions to Darcy’s Law. PhD thesis Delft University of Technology, Netherlands
- Bader S, Kooi H (2005) Modelling of solute and water transport in semi-permeable clay membranes: comparison with experiments. *Adv Water Res* 28:203–214
- Barbour SL, Fredlund DG (1989) Mechanisms of osmotic flow and volume change in clay soils. *Can Geotech J* 26:551–562
- Benson C, Daniel D (1990) Influence of clods on the hydraulic conductivity of compacted clay. *J Geotech Eng* 116:1231–1248
- Cao G, Zheng C, Scanlon BR, Liu J, Li W (2013) Use of flow modeling to assess sustainability of groundwater resources in the North China Plain. *Water Resour Res* 49:159–175
- Cey BD, Barbour SL, Hendry MJ (2001) Osmotic flow through a Cretaceous clay in southern Saskatchewan, Canada. *Can Geotech J* 38:1025–1033
- Daniel DE (1984) Predicting hydraulic conductivity of clay liners. *J Geotech Eng-ASCE* 110:285–300
- Datta B, Vennalokanti H, Dhar A (2009) Modeling and control of saltwater intrusion in a coastal aquifer of Andhra Pradesh, India. *J Hydro-Environ Res* 3(3):148–159
- Dunn RJ, Mitchell JK (1984) Fluid conductivity testing of fine-grained soils. *J Geotech Eng-ASCE* 110:1648–1665
- Fei J (1988) Groundwater resources in the North China Plain. *Environ Geol Water Sci* 12:63–67
- Fritz SJ (1986) Ideality of clay membranes in osmotic processes—a review. *Clay Clay Miner* 34:214–223
- Fritz SJ, Marine IW (1983) Experimental support for a predictive osmotic model of clay membranes. *Geochim Cosmochim Acta* 47:1515–1522
- Garavito AM, Bader S, Kooi H, Richter K, Keijzer TJS (2002) Numerical modelling of chemical osmosis and ultrafiltration across clay membranes. *Comput Method Water Resour* 47:647–653
- Garavito AM, Kooi H, Neuzil CE (2006) Numerical modeling of a long-term in situ chemical osmosis experiment in the Pierre Shale, South Dakota. *Adv Water Resour* 29:481–492
- Ghassemi A, Diek A (2003) Linear chemo-poroelasticity for swelling shales: theory and application. *J Petrol Sci Eng* 38:199–212
- Greenberg JA, Mitchell JK, Witherspoon PA (1973) Coupled salt and water flows in a groundwater basin. *J Geophys Res* 78:6341–6353
- Hanshaw BB (1971) Natural membrane phenomena and subsurface waste emplacement. *AAPG Bull* 55:2085
- Hanshaw BB, Hill GA (1969) Geochemistry and hydrodynamics of paradox basin region Utah Colorado and New Mexico. *Chem Geol* 4:263
- Hart M, Whitworth TM, Atekwana E (2008) Hyperfiltration of sodium chloride through kaolinite membranes under relatively low-heads—implications for groundwater assessment. *Appl Geochem* 23:1691–1702
- Henning JT, Evans JC, Shackelford CD (2006) Membrane behavior of two backfills from field-constructed soil-bentonite cutoff walls. *J Geotech Geoenviron* 132:1243–1249
- Kang J, Shackelford CD (2009) Clay membrane testing using a flexible-wall cell under closed-system boundary conditions. *Appl Clay Sci* 44:43–58
- Katzir-Katchalsky A, Curran PF (1965) Nonequilibrium thermodynamics in biophysics. Harvard University Press, Cambridge
- Keijzer T (2000) Chemical osmosis in natural clayey material. Utrecht University, pp 57–64
- Keijzer T, Loch J (2001) Chemical osmosis in compacted dredging sludge. *Soil Sci Soc Am J* 65:1045–1055
- Keijzer T, Kleingeld PJ, Loch J (1999) Chemical osmosis in compacted clayey material and the prediction of water transport. *Eng Geol* 53:151–159
- Kemper WD, Rollins JB (1966) Osmotic efficiency coefficients across compacted clays. *Soil Sci Soc Am P* 30:529
- Kharaka YK, Berry F (1974) Influence of geological membranes on geochemistry of subsurface waters from Miocene sediments at Kettleman north dome in California. *Water Resour Res* 10:313–327
- Kooi H, Garavito AM, Bader S (2003) Numerical modelling of chemical osmosis and ultrafiltration across clay formations. *J Geochem Explor* 78–9:333–336
- Loch JG, Richter K, Keijzer TJ (2005) Coupling between chemical and electrical osmosis in clays. IUTAM Symposium on Physicochemical and Electromechanical Interactions in Porous Media. Springer, pp 283–288
- Loch JG, Lima AT, Kleingeld PJ (2010) Geochemical effects of electro-osmosis in clays. *J Appl Electrochem* 40:1249–1254
- Malusis MA, Shackelford CD (2002) Theory for reactive solute transport through clay membrane barriers. *J Contam Hydrol* 59:291–316
- Malusis MA, Shackelford CD (2004) Predicting solute flux through a clay membrane barrier. *J Geotech Geoenviron* 130:477–487
- Malusis MA, Shackelford CD, Olsen HW (2003) Flow and transport through clay membrane barriers. *Eng Geol* 70:235–248
- Marine IW, Fritz SJ (1981) Osmotic model to explain anomalous hydraulic heads. *Water Resour Res* 17:73–82
- Neuzil CE (2000) Osmotic generation of ‘anomalous’ fluid pressures in geological environments. *Nature* 403:182–184

- Noy DJ, Horseman ST, Harrington JF, Bossart P, Fisch HR (2004) An experimental and modelling study of chemico-osmotic effects in the Opalinus Clay of Switzerland. Mont Terri Project—Hydrogeological Synthesis, Osmotic Flow. Geology Series. Federal Office for Water and Geology, Bern, Switzerland: 95–126
- Oduor P, Whitworth TM (2004) Transient modeling of hyperfiltration effects. *Math Geol* 36:743–758
- Oduor PG, Santos XT, Casey FX (2009) Solute exclusionary properties of porous shale wafers. *J Porous Media* 12:501–518
- Olsen HW (1969) Simultaneous fluxes of liquid and charge in saturated kaolinite. *Soil Sci Soc Am P* 33: 338
- Olsen HW (2003) Coupled chemical and liquid fluxes in earthen materials *Geotechnical Special Publication*: 57–85
- Olsen HW, Gui S, Lu N (2000) Critical review of coupled flow theories for clay barriers. *Transp Res Rec J Transp Res Board* 1714:57–64
- Sherwood JD, Craster B (2000) Transport of water and ions through a clay membrane. *J Colloid Interf Sci* 230:349–358
- Soler JM (2001) The effect of coupled transport phenomena in the Opalinus Clay and implications for radionuclide transport. *J Contam Hydrol* 53:63–84
- Takeda M, Hiratsuka T, Manaka M, Finsterle S, Ito K (2014) Experimental examination of the relationships among chemico-osmotic, hydraulic, and diffusion parameters of Wakkanai mudstones. *J Geophys Res Solid Earth* 119:4178–4201
- Wang S, Shao J, Song X, Zhang Y, Huo Z, Zhou X (2008) Application of MODFLOW and geographic information system to groundwater flow simulation in North China Plain, China. *Environ Geol* 55:1449–1462
- Wang S, Song X, Wang Q, Xiao G, Wang Z, Liu X, Wang P (2012) Shallow groundwater dynamics and origin of salinity at two sites in salinated and water-deficient region of North China Plain, China. *Environ Earth Sci* 66:729–739
- Yeo S, Shackelford C, Evans J (2005) Membrane behavior of model soil-bentonite backfills. *J Geotech Geoenviron* 131:418–429
- Yeung AT (1990) Coupled flow equations for water, electricity and ionic contaminants through clayey soils under hydraulic, electrical and chemical gradients. *J Non-Equil Thermody* 15:247–267
- Yeung AT, Mitchell JK (1993) Coupled fluid, electrical and chemical flows in soil. *Geotechnique* 43:121–134